Synthetic Sequence Effects in Polyurethane–Poly(*n*-Butyl Methacrylate) Mixtures: Grafting and Mechanical Properties

R. B. FOX, J. P. ARMISTEAD, C. M. ROLAND, and D. J. MOONAY,
Polymeric Materials Branch, Naval Research Laboratory, Washington, D.C. 20375-5000

Synopsis

Morphology, stress–strain properties, and grafting have been investigated in highly phase-separated polyurethane (PU)–poly(*n*-butyl methacrylate) (PBMA) mixtures as a function of the sequence of formation of the components, both linear (*l*) and crosslinked (*x*), in the presence of each other. In the range of 0.3–0.7 weight fraction of PU, a morphology of PBMA particles in a PU matrix results. Particle size depends on matrix viscosity at the time of PBMA formation, decreasing as viscosity increases. The PBMA(*l*) particles are spherical; PBMA(*x*) particles are irregular in shape when formed in a fluid medium but tend to become spherical as the delay time before the onset of their formation is increased. Grafting, decreasing with increasing delay time, is observed between PBMA(*l*) particles and the PU(*x*) or PU(*l*) matrix. The grafting results from transesterification between BMA and the polyol precursors to the PU. Two families of mechanical properties are found, depending generally more on particle shape than size. Systematic trends of property values through a series of samples of constant composition, but increasing delay times, are observed with greater variation in the series with PBMA(*x*) particles; the trends are explainable in terms of matrix immobilization by the particles.

INTRODUCTION

In our previous reports,[1,2] dynamic mechanical and some related properties were described for essentially immiscible combinations of a polyol-based polyurethane (PU) and poly(n-butyl methacrylate) (PBMA) having one, both, or neither component crosslinked. These combinations, with *l* for linear and *x* for crosslinked and the PU given first, are designated by *lx, xl, xx,* or *ll,* respectively. For each combination, a series of materials were prepared from mixtures of the reactants by photopolymerization of the PBMA precursors at various times during a slow dibutyl tin dilaurate (DBTDL)-catalyzed polymerization of the PU precursors at room temperatures. Within the 0.3–0.7 PU weight fraction range, a morphology of PBMA particles in a continuous PU matrix was found. Particle size decreased as the delay time increased between the PU and the PBMA initiation. Crosslinking the PBMA resulted in irregularly-shaped particles, while spherical particles formed in the absence of crosslinker. Initial moduli and dynamic mechanical properties varied continuously with delay time, with a minimum midway during the PU formation; these effects were more pronounced in the series with irregular particles. As particle size decreased in the *xx* series, the temperature of the loss tangent maximum corresponding to PBMA gradually decreased while that for PU remained nearly constant, sug-

Journal of Applied Polymer Science, Vol. 41, 1281–1298 (1990)

CCC 0021-8995/90/5-61281-18$04.00

gesting the formation of a PBMA phase enriched by PU or the increasing influence of the interface with the PU continuum. A similar effect was observed in the other three series, but only when particle sizes became less than 0.1 μm. No relationship was adduced between these T_g decreases and changes in the properties reported here. Precursor diluent effects were suggested as the origin of many of the property and structure changes resulting from altering the sequence of component formation.

Our purpose in this report is to enlarge on those findings, with a focus on stress-strain properties and their relationships to morphology and the dynamic mechanical properties. Further, we will extend our preliminary observations[2] of grafting processes in the *xl* series of materials.

EXPERIMENTAL

Materials

As described previously,[2] the PU precursor materials were Adiprene L-100 (Uniroyal, Inc.), a poly(oxytetramethylene glycol) capped with toluene diisocyanate, NCO eq mol wt 1030; 1,4-butanediol (BD) and 1,1,1-trimethylolpropane (TMP); and, as catalyst, DBTDL. Acrylic precursors included n-butyl methacrylate (BMA), washed with 10% aq NaOH to remove inhibitor; tetramethylene glycol dimethacrylate (TMGDM) crosslinker; and benzoin *sec*-butyl ether (BBE) as a photosensitizer. These materials were dried appropriately but not otherwise purified.

Sample Preparation

For each of the *xx*, *lx*, and *xl* mixtures, three PU : PBMA compositions, 3 : 7, 5 : 5, and 7 : 3, were made; with the *ll* mixture, only the 5 : 5 composition was prepared. An equivalent weight ratio of 0.95 for OH : NCO was maintained for the PU components; a 3.5 : 1 (by weight) BD : TMP mixture was used for the PU(x) samples. Samples containing PBMA(x) were made with a 60 : 1 (mole ratio) BMA : TMGDM mixture. These ratios yield a calculated M_c of 1700 and 4200 g/mol for the PU(x) and PBMA(x), respectively. In each mixture, 0.05 wt % DBTDL, based on the total sample weight, and 0.1% BBE, based on the weight of the BMA, were used as catalysts.

For a given composition, a mixture of appropriate weights of all of the precursors except DBTDL was stirred until it was homogeneous. After thorough degassing of the mixture, the DBTDL was added and the time, t_0, noted. Following a second, brief, degassing, the mixture was transferred to a series of cells composed of thin glass plates faced by Teflon shim stock, separated by a 1 mm gasket, and held together by spring clamps. After a suitable interval, t_i-t_0, each cell was suspended for 2 h in a Rayonet Photoreactor fitted with UV sources nominally rated at 300 nm. The temperature within the photoreactor was about 30°C; all other operations were conducted at room temperature, 23°C. About 24 h after t_0, each cell was disassembled and the sheet product heated at 90°C in vacuum for 48 h. Small weight losses at any step were assumed to be BMA and were taken into account in calculating the composition of the sample.

Reference polymers and networks were prepared by analogous procedures. Two PU networks were made, one from the precursors alone and the other in the presence of 50 wt % of BMA, which was subsequently removed by evaporation.

Characterization

Dynamic mechanical characterization was carried out with an automated Rheovibron DDV-IIC (IMASS) in the tensile mode with a heating rate of 1.5°C/min; data taken at 11 Hz are reported here. The same sample was used for the entire temperature range of −100–150°C. Because of the magnitude of the load cell compliance, properties of our samples in the glassy region below about −40°C were not viewed in any quantitative sense.

Stress–strain properties at room temperature were obtained with an Instron Model 4206 at a strain rate of 2/min; ASTM D638 type V specimens were used. Initial moduli are reported as the maximum moduli, E_{max}, shown in the low-strain portion of the stress-strain curve; yield stress values are the stresses corresponding to E_{max}.

Transmission electron micrographs were obtained from 125–250 nm sections dry cut on a Reichert Ultracut ultramicrotome with a FC4D cryostatic unit; temperatures were −100°C for the specimen and −80°C for the diamond knife. Sections stained with RuO_4 vapor as well as unstained sections were viewed by means of a Zeiss EM10 electron microscope. Particle areas in the micrographs were measured with the aid of a Quantex QX7 image enhancer with particle counting software.

RESULTS AND DISCUSSION

Mechanical and other properties for each series, as well as the component polymers, are given in Tables I–III; series designations, such as *lx*-.3, refer to a composition with a nominal PU weight fraction of 0.3. Dynamic properties of these series were cited in our earlier paper.[2]

Grafting

Extraction of the linear components from this system was more difficult than expected for mixtures formed by blending of components without specific interaction. Our PU (*l*) was soluble in DMF at 80°C, but in refluxing THF only about 5% by weight was dissolved after 24 h. Our PBMA (*l*) was readily soluble in DMF, THF, PhMe, CH_2Cl_2, and $CHCl_3$, but not in DMSO. The essential observations with the 5 : 5 mixtures were:

***xl*-.5.** Extraction with THF for 7000 h at room temperature produced sol fractions of 5, 12, and 34% of the weight corresponding to that calculated for PBMA (*l*) for samples aged one year with delay times of 13, 548, and 1539 min, respectively. Refluxing chloroform after 5000 h also produced a sol fraction corresponding to 34% of the expected weight of PBMA (*l*) from the 1538 min sample. Freshly made *xl*-.5 samples gave similar results but with higher sol fractions; infrared spectra indicated the presence of both PU and PBMA in these extracts.

TABLE I
Properties of the 5 : 5 Compositions

$t_i - t_0$ (min)	E_{max} (MPa)	Tensile strength (MPa)	Break strain multiple	Toughness (σ–ϵ area) (MPa)	Yield stress (MPa)	Particle diameter (μm)	SD (μm)
			Series *lx*				
16	11.9	15.2	9.3	83	3.0	0.49	0.63
137	9.0	16.3	10.6	93	2.4	0.26	0.34
258	8.4	16.2	11.9	100	1.9	0.24	0.22
389	5.0	16.8	13.6	114	1.0	0.12	0.04
674	7.2	17.3	14.4	114	1.0	0.10	0.016
1284	7.8	14.5	13.8	99	1.1	0.071	0.013
			Series *xl*				
13	3.7	18.7	16.2	141	0.45	0.71	0.98
133	3.0	19.4	17.4	148	0.4	0.41	0.34
548	2.5	17.5	18.0	136	0.4	0.27	0.12
1247	2.7	15.3	18.0	122	0.3	0.13	0.036
1539	3.3	15.4	18.0	122	0.3	0.11	0.031
			Series *xx*				
15	12.0	14.6	7.6	63	1.7	0.38	0.80
76	8.8	16.4	8.4	72	1.4	0.27	0.30
197	8.5	16.8	8.7	73	1.0	0.22	0.28
586	4.7	19.3	11.1	97	0.7	0.10	0.10
1286	6.6	16.9	10.8	83	0.8	0.063	0.01
1508	7.1	16.0	10.4	78	0.9	0.063	0.01
			Series *ll*				
22	4.6	22.0	16.5	157	1.3	0.42	0.63
145	3.8	22.4	16.9	160	1.2	0.28	0.26
266	3.5	22.6	17.2	162	1.25	0.17	0.11
925	5.1	21.2	17.2	153	1.5	0.13	0.037
1466	6.9	18.2	16.1	129	1.5	0.096	0.023

***lx*-.5.** Extraction with DMF at 80°C produced a sol fraction corresponding to 99 and 95% of the calculated weight of PU(*l*) for samples with delay times of 53 and 1257 min, respectively. No PBMA was detected in the infrared spectra of these extracts.

***ll*-.5.** Both aged and fresh samples were soluble in DMF at 75°C. With a freshly prepared sample having a delay time of 62 min, refluxing THF extracted only 8% of the amount calculated for PBMA(*l*), while toluene at 70 or 90°C extracted only 16%. For a sample with a delay time of 1404 min, refluxing THF extracted 90% of the weight corresponding to PBMA(*l*). Again, infrared spectra of the extracted materials indicated the presence of a PU; no unreacted isocyanate was found.

These observations are consistent with grafting if the reasonable assumption can be made that PU(*l*)-*g*-PBMA(*l*) is less soluble in most PBMA solvents than PBMA(*l*) itself. The finding of full solubility of *ll*-.5 in DMF mitigates

against crosslinking of PBMA as a source of poor solubility. Alternative explanations may involve pseudo-crosslinking resulting from crystallization in the PU somehow trapping PBMA or strong hydrogen bonding between >NH in the PU and >C=O in the PBMA. From DSC and WAXS data, little crystallization exists in our PU, and infrared spectra provide no evidence of hydrogen bonding involving the PBMA in these mixtures.

If, indeed, grafting (i.e., the formation of PU(*l*)-*g*-PBMA(*l*), PU(*l*)-*g*-PBMA(*x*), or PU(*x*)-*g*-PBMA(*l*)) is responsible for the extraction results, account must be made for the apparent decrease in grafting as delay time increases in the *xl* and *ll* series, as well as for the full extraction of PU(*l*) from both short and long delay samples in the *lx* series. As delay time increases, the BMA (and the photosensitizer BBE) will be in contact with the PU precursors (L-100, polyols, and DBTDL) in the dark for increasing time periods during which the precursors are reacting to form PU before photopolymerization is initiated. In an experiment in which delay time was "infinite," carried out by allowing precured PU(*x*) to imbibe a mixture of BMA, BBE, and DBTDL and photopolymerizing the swollen specimen, 62% of the weight calculated for PBMA(*l*) was easily extractible by refluxing THF. Therefore the grafting reaction must occur more readily with the PU precursors than with the PU itself. Insolubilization of the PBMA(*l*) does require the combination of DBTDL and light, since (a) PBMA(*l*) was fully extractible from an *xl* sample prepared in the absence of DBTDL by first photopolymerizing the BMA and then thermally curing the PU(*x*); and (b) an *xl* precursor mixture containing DBTDL and cured in the dark was found to incorporate less than 5% of the initial BMA.

Of the remaining reactants, diisocyanates are not known to react directly with acrylic monomers such as BMA. Irradiation of a mixture of L-100, BMA, BBE, and DBTDL, extraction with dimethyl sulfoxide, dissolution in THF, and precipitation into methanol provided material the infrared spectrum of which showed the presence only of PBMA.

By elimination, the polyols are implicated in the presumed grafting process. This was confirmed by the following "test tube" experiments. Irradiation of a two-phased mixture of BD and BMA produced an immediate viscosity increase in both layers, and the viscosity of the BMA layer also increased further on standing in the dark. The reaction products from both layers were fully soluble in THF. However, irradiation of a BD-BMA mixture containing added DBTDL produces a gel that is insoluble in THF, indicating the formation of crosslinked material. This reaction was accelerated by BBE. It is suggested that in the

TABLE II
Properties of Component Polymers

	E_{max} (MPa)	Tensile strength (MPa)	Break strain multiple	Toughness (σ–ϵ area) (MPa)
PU (*l*)	0.86	15.7	31.5	173
PU (*x*)	1.1	13.5	20.7	110
PBMA (*l*)	204	14.3	4.5	54
PBMA (*x*)	198	15.4	1.8	27

TABLE III
Properties of the 3 : 7 and 7 : 3 Compositions

$t_i - t_0$ min	Initial modulus MPa	Tensile strength MPa	Break strain multiple	Toughness (σ–ϵ area) MPa
		Series *lx*-.3		
2	21.3	11.3	4.9	41
124	21.3	14.5	6.4	60
252	18.2	13.4	6.4	57
371	16.6	12.3	6.6	55
677	10.8	12.6	9.2	74
1528	15.1	7.6	8.2	47
		Series *lx*-.7		
1	4.3	22.4	19.2	202
129	2.1	24.4	21.9	221
261	1.8	26.1	25.7	260
385	1.6	20.1	25.9	201
710	2.3	23.0	26.0	220
1309	2.3	20.8	26.2	199
1601	2.6	18.6	24.7	169
		Series *xl*-.3		
1	6.0	12.5	10.4	75
123	5.5	15.0	12.0	95
245	5.2	14.6	11.5	91
647	5.0	12.1	10.5	72
1338	4.7	10.3	10.1	61
1630	4.9	10.2	10.5	63
		Series *xl*-.7		
1	1.9	18.4	20.0	153
134	1.6	19.7	23.3	195
286	1.5	12.8	18.8	104
599	1.4	15.3	23.6	146
1308	1.6	16.8	26.3	194
1575	2.0	12.5	19.7	99
		Series *xx*-.3		
10	21.5	10.9	4.7	39
139	22.4	12.0	4.8	41
262	21.1	11.9	4.8	40
563	14.0	11.3	5.5	40
1868	9.6	12.0	7.4	56
2134	10.7	11.3	6.7	47
2784	15.3	11.2	6.4	45
		Series *xx*-.7		
18	4.5	19.7	16.4	152
139	1.8	20.8	19.2	170
259	1.5	19.4	20.7	162
669	1.9	17.7	20.0	138
1272	2.0	18.1	22.1	153
1512	2.1	17.7	21.8	152

presence of DBTDL at least some of the BD has been converted by ester exchange to a dimethacrylate which can act as a crosslinker during the photopolymerization of the BMA. Under our conditions, DBTDL was found to have little qualitative effect on the rate of photopolymerization of BMA.

We conclude that the insolubilization of PBMA(*l*) has its origin in a DBTDL-catalyzed phototransesterification reaction between BMA and the polyols. Support for this contention is found in the work of Poller and Retout,[3] who reported that tin compounds, including dibutyltin diacetate, were effective catalysts for the transesterification of *n*-propyl acetate with methanol. In our PU/PBMA system, the greatest effect would occur in the presence of trimethylol propane (TMP), which is the triol used in forming PU(*x*) in the *xl* and *xx* series; in the latter series, little extractable material would be expected in any case.

A grafting process involving transesterification necessarily consumes polyol hydroxyl groups that would otherwise react to form part of the PU network. Byproduct butanol will react with isocyanate ends, resulting in dangling PU chains. However, since a single transesterification event can accomodate a large number of BMA molecules, the effect of grafting on the crosslink density of the PU (*x*) may be quite small. On the other hand, if more than one hydroxyl group in a BD or TMP molecule undergoes transesterification, crosslinking in the PBMA graft may also occur. The sum of these effects may be minor relative to the expected decrease in crosslink density with increasing delay time that results from the PU being formed at the expense of PBMA precursors. Support for this contention is seen in our observation[2] that recoverable compliance in the *xl* series increases with delay time, which implies that overall crosslink density is decreasing.

A possible role for TMGDM in hindering transesterification or the grafting process may be considered in light of the fact that grafting was observed only in the absence of TMGDM. Transesterification between polyol hydroxyl groups and BMA or TMGDM can lead to one and two species, respectively, capable of acting as graft sites. In that sense, TMGDM would be expected to enhance, rather than hinder, grafting; at the low concentrations of TMGDM used, this effect must be very small. However, TMGDM may play a far larger indirect role in the transesterification process by reducing the concentration of unreacted BMA through its preferential dissolution in the PBMA–TMGDM network as it forms. The rate of network formation by a free radical process is likely to exceed that of the ionic process of transesterification. At the same time, any grafting process involving PBMA chain ends will also be reduced by PBMA network formation.

The absence of grafting has been reported[4,5] for related polyurethane–poly(methyl methacrylate) mixtures in which the polyurethane was formed prior to the polymerization of the acrylate. While there were differences in detail, conditions were generally equivalent to the long delay times used in our work, and therefore little grafting would be expected.

Morphology

Within the composition range studied, all samples were shown by TEM to have a morphology of PBMA particles in a continuous PU matrix. The finding[2]

of no permanent set in the *xl* series supports the TEM results. This agrees with the usual experience that the polymer formed first will be a continuous phase, since the PU precursor is itself a polymer; PBMA is immiscible with this precursor. Examples of TEM for some of the series were presented in our earlier work.[1,2] In each case, particle size decreased with increasing delay time before PBMA initiation. The *xl* and *ll* series have spherical PBMA particles for any delay time. In contrast, the *lx* and *xx* series exhibit an irregular PBMA particle morphology for short delay times, with increasingly smooth-surfaced particles and eventually spherical particles forming as delay time increases. Micrographs of samples having the shortest and longest delay times in each of the 5 : 5 series are shown in Figures 1 and 2. A hint of large irregular particle interconnectivity

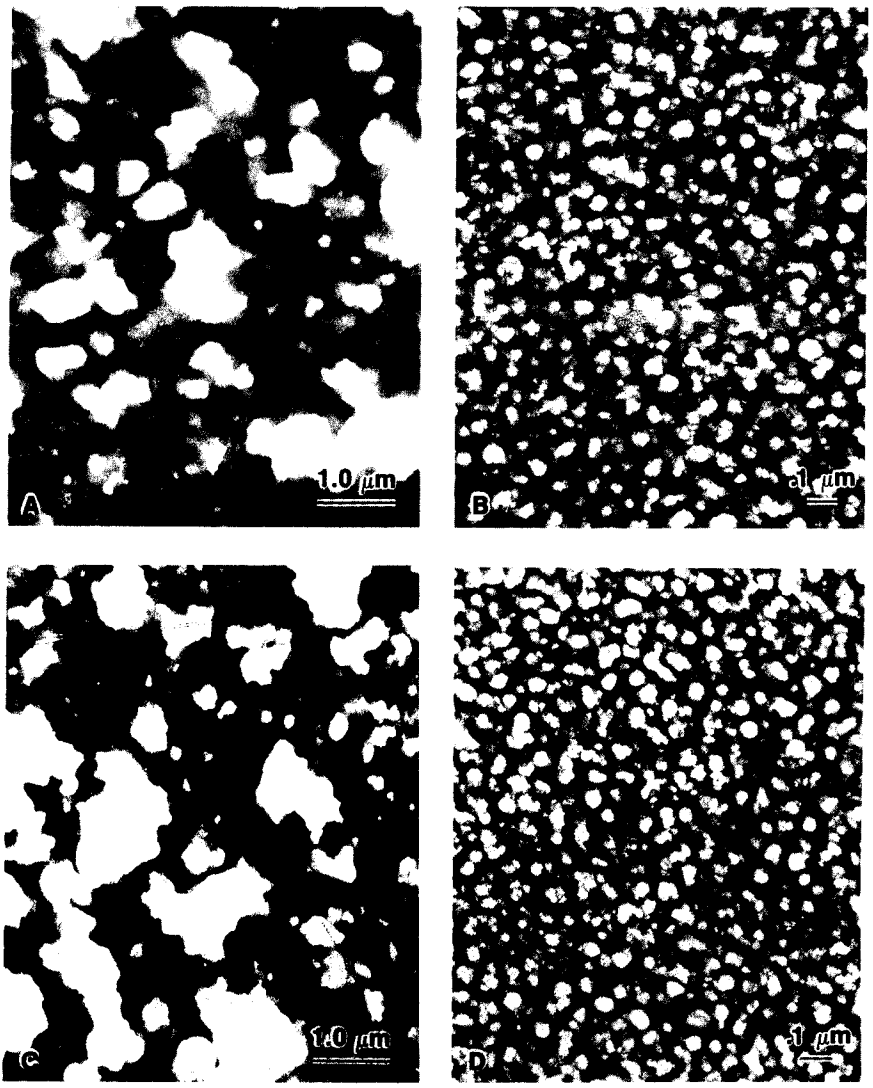

Fig. 1. TEM micrographs from the *lx*-.5 series: (a) 16 min delay; (b) 1286 min delay; *xx*-.5 series: (c) 15 min delay; (d) 1508 min delay.

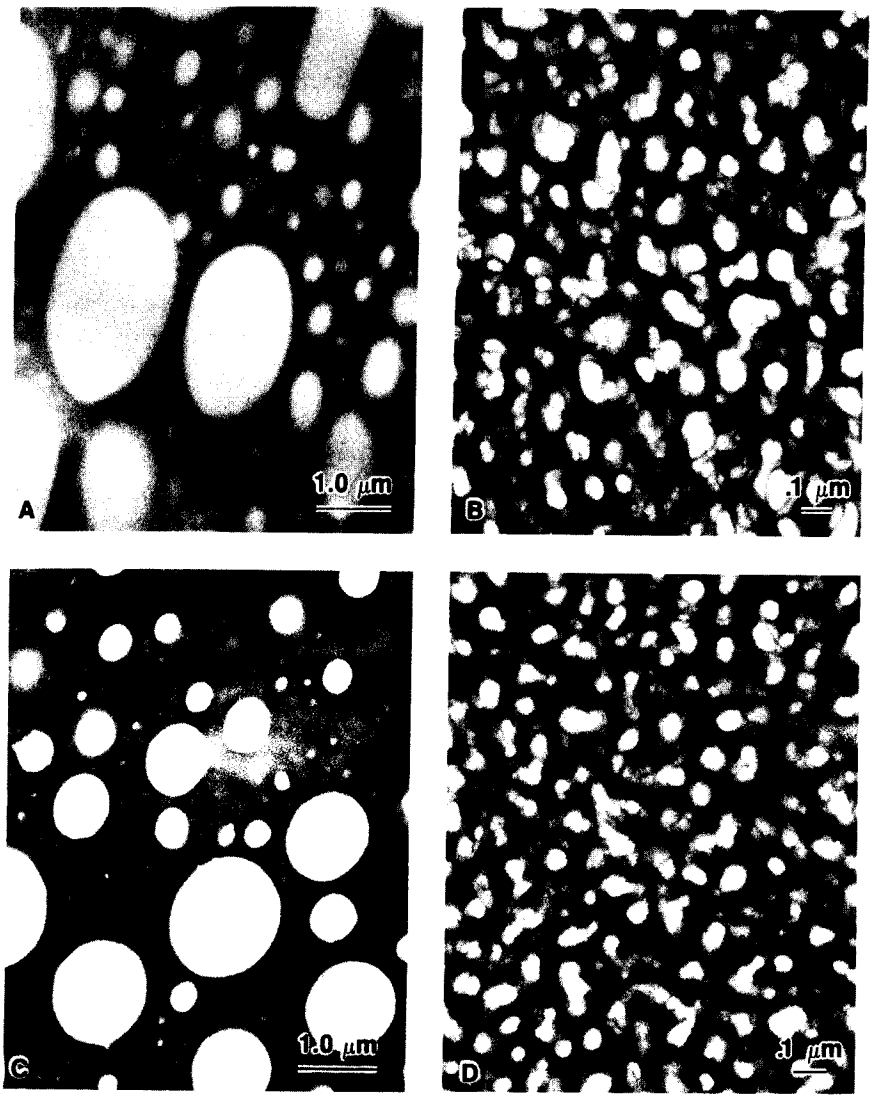

Fig. 2. TEM micrographs from the *xl*-.5 series: (a) 13 min delay; (b) 1539 min delay; *ll*-.5 series: (c) 22 min delay; (d) 1466 min delay.

can be seen in the *lx* and *xx* series. Occlusions within particles were not observed. The same two families of materials seen in the micrographs are also seen in the trends in mechanical properties. Clearly, particle shape is an important factor in determining the properties exhibited by each family of materials.

While the qualitative particle size variation within each series is easy to see, absolute sizes and their distributions are another matter. In our previous papers,[1,2] sizes were estimated visually by counting particles seen in the micrographs; necessarily, this procedure emphasized large particles. In Table I, the particle diameters cited were obtained by the more rigorous counting procedures used in TEM work,[6] facilitated by automated image processing. Irregular particles were assumed to be spherical for the purpose of deducing diameters from

measured areas. Weight average diameters (the second moment of the number average) were used because the large number of small particles in a given sample tended to overly influence number average diameters. The broadness of the distributions are reflected in the standard deviations shown in Table I. Samples with short delay times showed bimodal particle size distributions, with a maximum at small particle diameters and a fairly broad and flat distribution through the larger particles. As delay time increased, the number and size of the larger particles decreased, until finally at long delay times only a peak at small particle diameters was observed. Such bimodality has also been reported[7] for epoxy/poly(*n*-butyl acrylate) interpenetrating networks in which the components were formed in roughly the same time frame. The bimodal distributions encountered in that work were taken as evidence that the larger particles were formed before matrix gelation and the smaller particles by continued phase separation after gelation. Our results agree with that interpretation.

Plots of dynamic properties, such as tan δ_{max} or the ratios of the high to low temperature tan δ_{max} peaks, against particle diameters are similar to plots of the same properties against delay times in that two families of property trends were apparent. This also holds true for the stress-strain properties reported in Table I and discussed below. The variation of E_{max} and the yield stress values with particle diameter are shown in Figures 3 and 4, respectively.

Inspection of Table I indicates that the failure properties are not a simple function of particle diameter or its reciprocal, which is proportional to specific surface area. Particles are therefore not acting as classical flaws. At the high

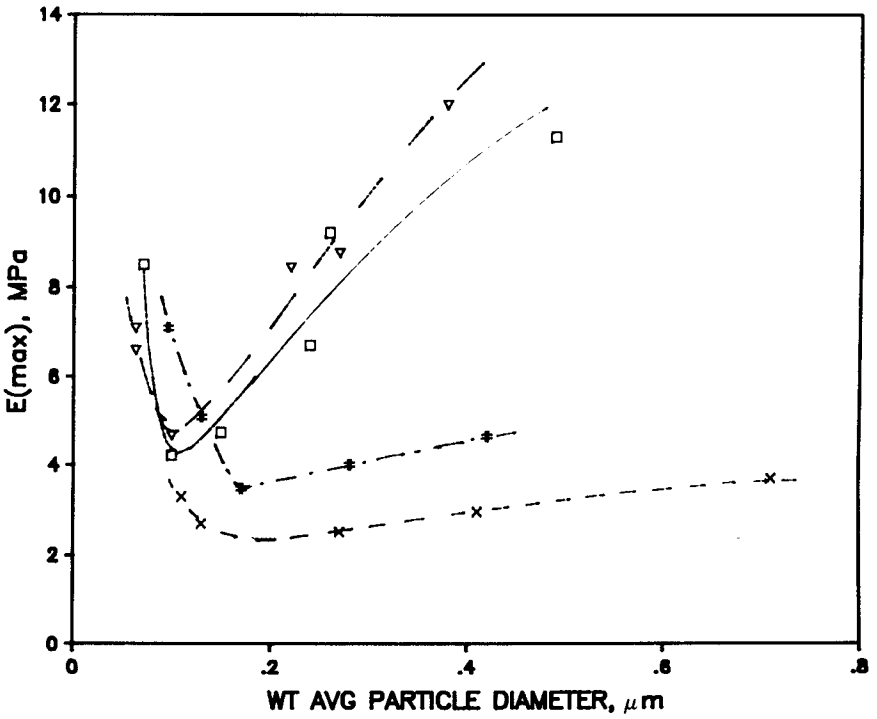

Fig. 3. Effect of PBMA particle diameter on tensile modulus maxima in 5 : 5 PU/PBMA mixtures: (□) *lx*; (×) *xl*; (▽) *xx*; (#) *ll*.

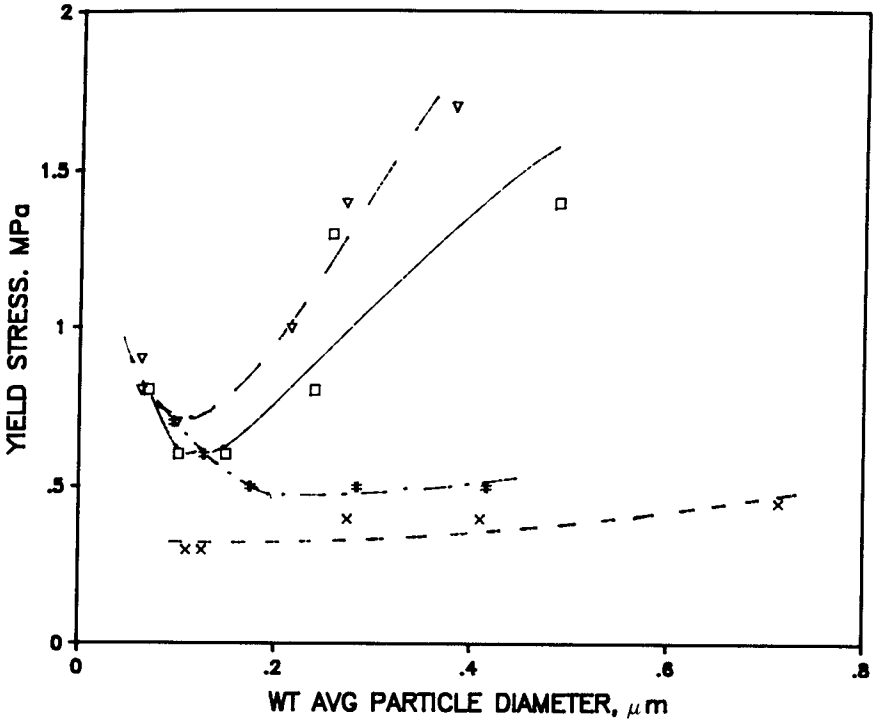

Fig. 4. Effect of PBMA particle diameter on yield stress in 5 : 5 PU/PBMA mixtures: (□) *lx*; (×) *xl*; (▽) *xx*; (#) *ll*.

end of the particle size scale, the *xl* and *ll* series, with spherical particles and grafting, have higher tensile strengths, ultimate elongations, and toughness than the corresponding *lx* and *xx* series with irregular particles. This is consistent with good adhesion through grafting, since, for example, in the absence of grafting the largest particles would be expected to decrease tensile strength.

Underlying causes for the formation of irregular particles are not clear. This morphology has been reported[7] for a single epoxy–poly(*n*-butyl acrylate) interpenetrating network polymer in which the components were formed simultaneously at approximately the same rate. In our work, the crosslinked particles were formed in a medium of relatively low viscosity that may provide conditions appropriate for proliferous polymerization not usually encountered in the absence of a crosslinker.

Stress–Strain Properties

Stress–strain properties are given in Tables I–III. Typical low-strain trends in the stress-strain curves are shown in Figures 5 and 6 for the *xx*-.5 and *xl*-.5 series, respectively. Curves for the *xx*-.5 series resemble those of the *lx*-.5 series. Both the *xx* and *lx* series of curves show distinct inflections at low strain that appear to be yield stress points. These stresses decrease with increasing delay time for the PBMA initiation after the onset of PU polymerization. Likewise, the curves for the *xl*-.5 series and the *ll*-.5 series are similar. In these two series, the yield stresses are not as pronounced as in the *lx* and *xx* series and are nearly

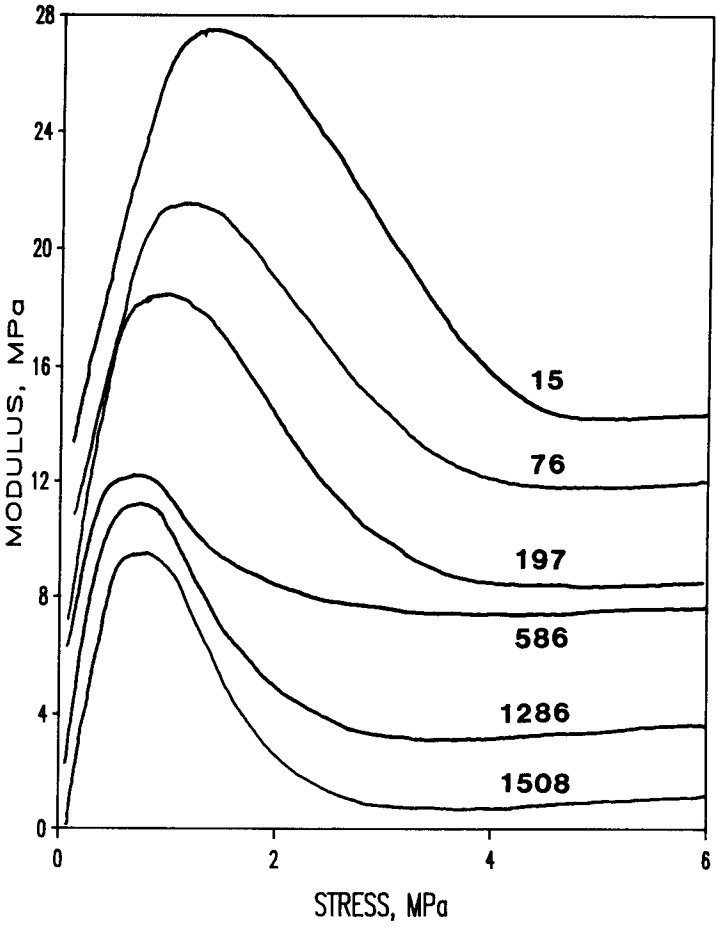

Fig. 5. Tensile moduli vs. stress at low strain in the *xx*-.5 series for various delay times (min); curves shifted vertically for clarity.

constant with increasing delay times. Trends in yield stress with delay time, shown in Figure 7, or with particle size (Fig. 4) clearly indicate two families of materials among the four component combinations in the 5 : 5 composition. Analogous results were found with the other compositions.

Stress-strain data were obtained at a temperature approximately midway between the temperatures of the tan δ_{max} of the PU (−17–−24°C) and the PBMA (58–72°C) phases in these strongly phase-separated materials. Undoubtedly the initial portions of the stress–strain curves reflect the contributions of the "glassy" PBMA phases at low strain. Yield stress values were generally proportional to the E_{max} and, for the *lx, xx* family, increased with increasing tan δ_{max} for the PBMA phase; the latter correlation was poor for the *xl, ll* family, however.

The E_{max} themselves are roughly proportional to the dynamic plateau storage moduli taken at 20°C and 11 Hz.[2] Further, while Figure 8 shows that E_{max} increase with decreasing tan δ_{max} for the PU phase with little differentiation among families, the corresponding plot, in Figure 9, of tan δ_{max} for the PBMA

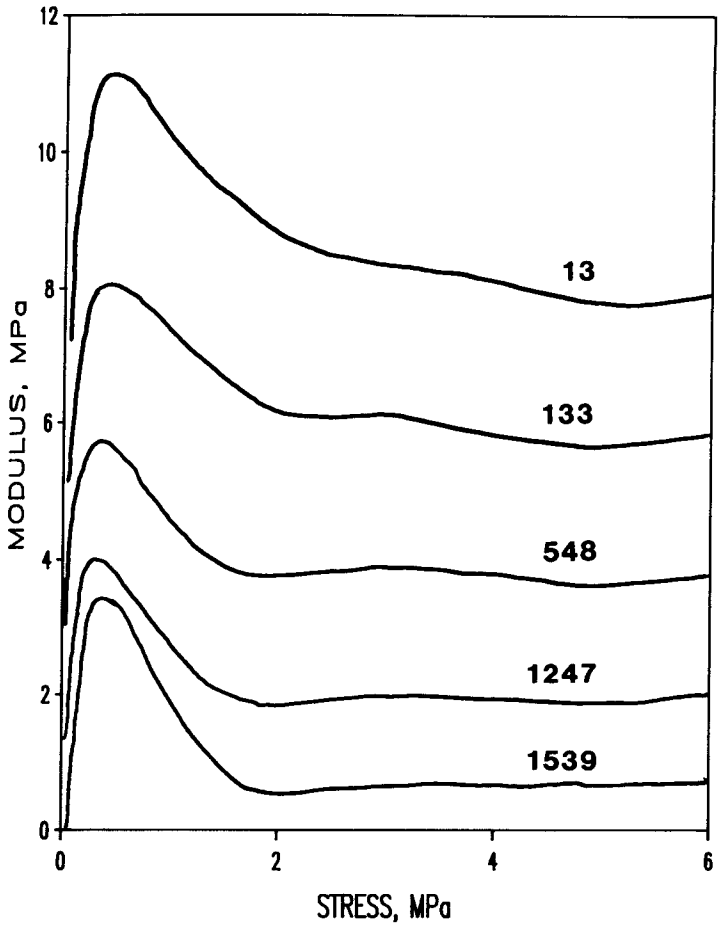

Fig. 6. Tensile moduli vs. stress at low strain in the *xl*-.5 series for various delay times (min); curves shifted vertically for clarity.

phase separates the families, pointing to the dispersed phase as the source of the groupings of stress–strain properties. As noted above, yield stresses increased with increasing PBMA domain size in the *lx, xx* family but were nearly independent of domain size in the *xl, ll* family. All of these trends are strongly suggestive of qualitatively different interactions between phases in the two families. With considerable scatter, tensile strength, break strain, and toughness (from the area under the stress-strain curve) each increase with increasing tan δ_{max} for the PU phase and decrease with increasing tan δ_{max} for the PBMA phase; families of data are not well-separated.

Familial relationships also appear in the trends of other stress-strain properties with delay time. The data for break strain are shown in Figure 10; a corresponding plot was presented earlier[2] showing that the E_{max} for the *lx* and *xx* series initially undergo a rapid decrease with increasing delay times while in the *xl* and *ll* series they are low and relatively constant.

There are not only trends with delay times within the series, but indications as well of general synergism in some properties relative to the individual com-

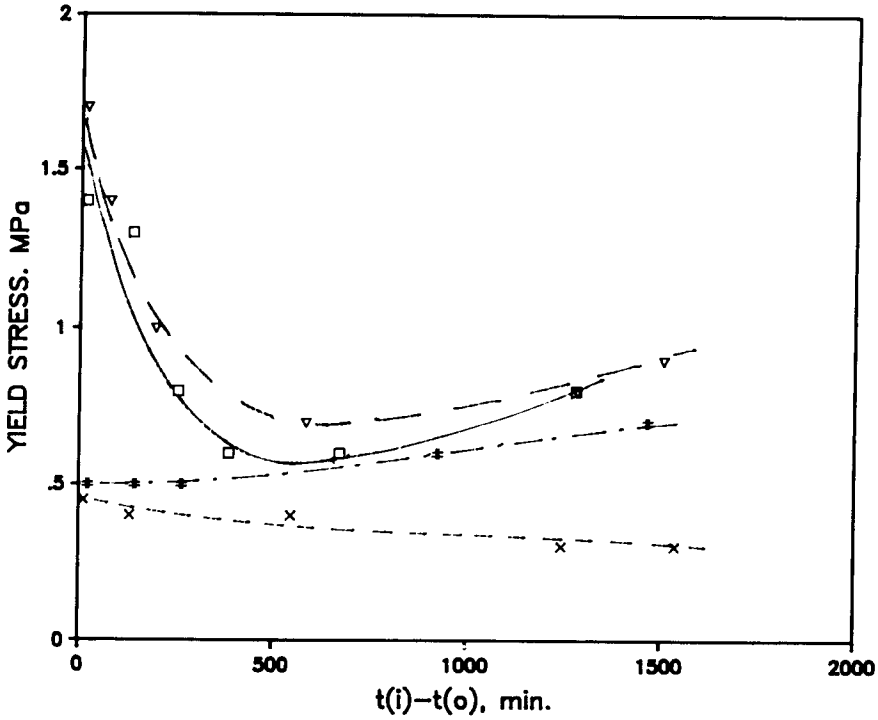

Fig. 7. Effect of delay time on yield stress in 5 : 5 PU/PBMA mixtures: (□) *lx*; (×) *xl*; (▽) *xx*; (#) *ll*.

ponent polymers. A typical example is shown in Figure 11, in which the highest values of tensile strength in each series are presented as a function of composition. Such synergism has been observed in the past for interpenetrating networks,[8] in which it was ascribed to an increase in crosslink density resulting from interpenetration.

The stress-strain properties reported here amplify and corroborate our earlier[2] conclusions that the observed synthetic sequence effects in the PU/PBMA system are largely a consequence of the state of dilution and viscosity of the medium in which the components are formed. As delay time before initiation of the PBMA increases, the PU is increasingly being formed in a mixture of PBMA precursors, resulting in a matrix with decreased modulus and, in the case of PU(x), lower crosslink density. Particle size is controlled by the viscosity of the reaction mixture at the time the PBMA particles were formed. Up to some critical PU matrix viscosity, particle shape is dictated by the presence or absence of crosslinking in the PBMA phase. Where the PBMA phase is crosslinked, i.e., in the *lx* and *xx* series, irregular particles are formed if the matrix is sufficiently mobile.

For a given PBMA volume and domain size, irregular particles present a greater matrix-particle interface area than do spherical particles. Consequently, a greater proportion of flexible matrix chains will be immobilized in proximity to the glassy phase. The larger effective particle size is equivalent to an increase in the effective volume fraction of the dispersed phase, and it will result in higher moduli under low strain, principally through strain amplification. As

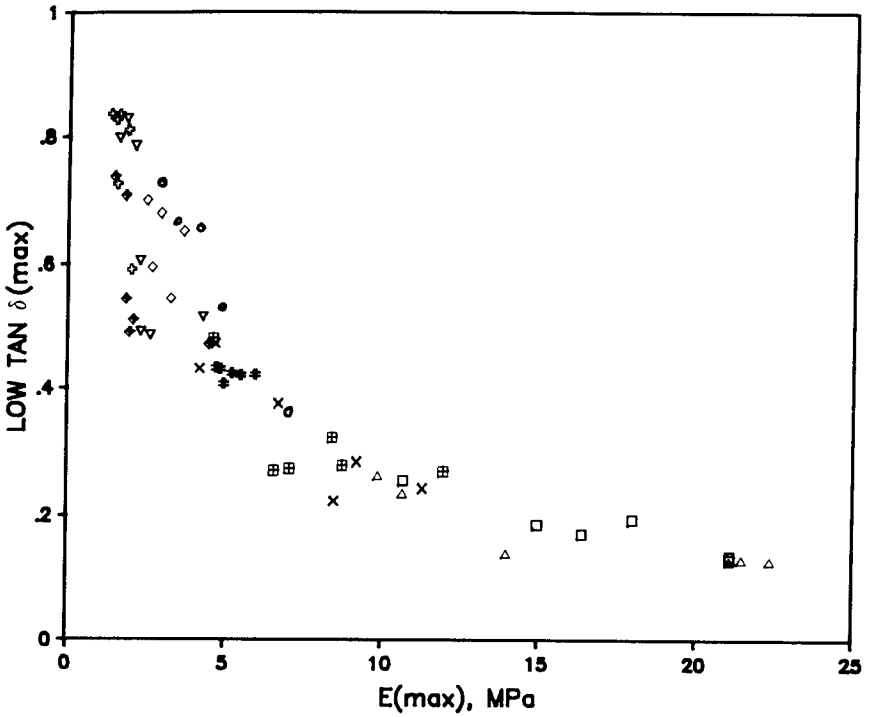

Fig. 8. Tensile modulus maxima vs. PU tan δ maxima (11 Hz) for all samples in Tables I and III.

delay time increases, the viscosity of the medium increases, and smaller and less irregular particles are formed. At a sufficiently long delay time, a morphology is produced that is similar to that formed in the absence of crosslinking. Spherical particles formed in the absence of crosslinking in the PBMA phase not only provide lower moduli but are further affected by the grafting process reported above. It is reasonable to suppose that grafted particles also present an increased effective particle size but that mixing of the interphase with the matrix results in greater adhesion and therefore more gradual and therefore less distinct yielding. As grafting decreases as delay time increases, at least in the *xl* series, the particles formed in both the presence and absence of crosslinking become similar in both size and shape, and yielding appears in all of the series at long delay times.

SUMMARY AND CONCLUSIONS

The sequence of formation of the individual components in a mixture of PU and PBMA precursors strongly affects the extent of grafting and the morphology of the resulting multicomponent polymers and these factors in turn control mechanical properties.

Extensive grafting takes place in the *xl* series; and it probably occurs in the *ll* series; little or no grafting occurred in the *lx* series. Grafting is thus associated with the absence of a crosslinker among the precursors for the PBMA phase.

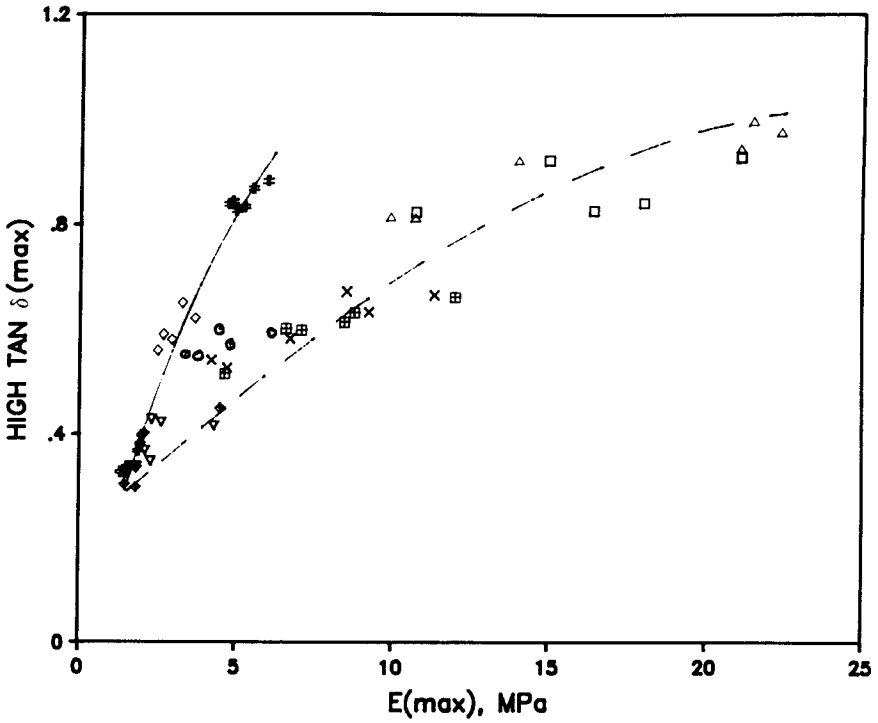

Fig. 9. Tensile modulus maxima vs. PBMA tan δ maxima (11 Hz) for all samples in Tables I and III: (——) *xl* series; (- - -) *lx* and *xx* series; (○) *ll*-.5.

The extent of the graft process was found to decrease as the concentration of polyol hydroxyl groups in the PU precursors decreases across a series. Transesterification accelerated by DBTDL and light is a likely mechanism for the process leading to graft sites.

Within the 0.3 to 0.7 PU weight fraction range, a morphology of PBMA(*l*) or PBMA(*x*) particles in a continuous PU matrix was found. Particle sizes decreased with increased delay time in all series and in the 5 : 5 compositions fell in the range of 0.06 μm to 0.7 μm on a weight average basis; these sizes are generally above the ranges for effective matrix reinforcement. Particle distributions were broad and tended to be bimodal at intermediate delay times, suggesting continued PBMA particle formation after cessation of irradiation. Two morphological families were observed through unequivocal TEM evidence. In the *xl* and *ll* series, spherical particles were found at all delay times. In the *lx* and *xx* series, irregular particles formed at short delay times; as delay times increased, irregularity lessened and shapes became increasingly spherical. Thus, spherical particles tend to be formed in all four series when irradiation begins after a critical matrix viscosity has been reached.

Family groups corresponding to morphologies were reflected in stress-strain property trends through each series, particularly at the short delay times where the PU matrix viscosity is relatively low and the largest particles were observed. The series with spherical particles had higher break strains, ultimate elongations, and toughness values, and lower E_{max} than the series with irregular par-

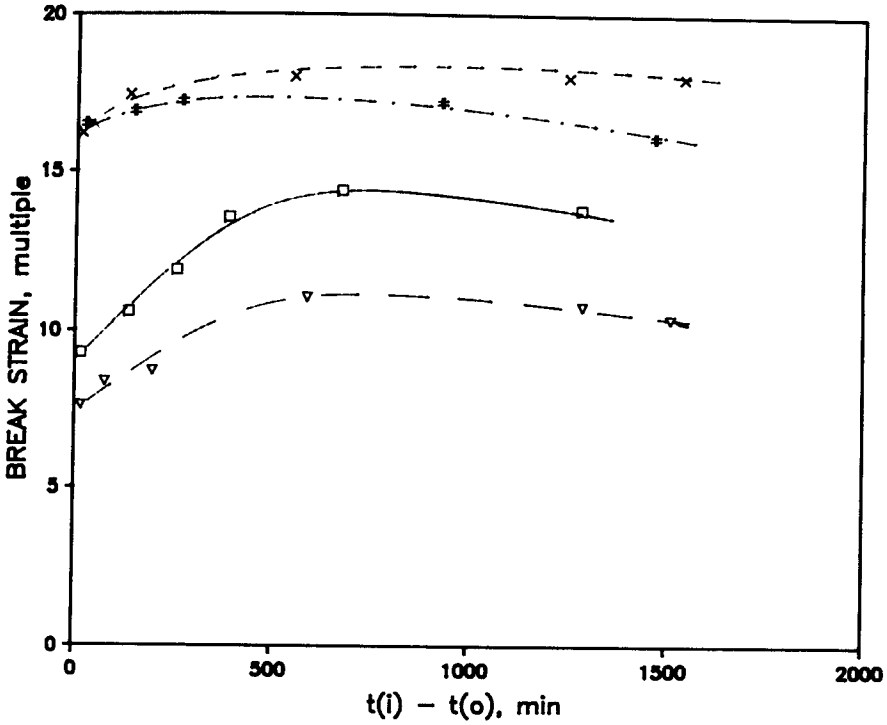

Fig. 10. Effect of delay time on break strain in 5 : 5 PU/PBMA mixtures: (□) *lx*; (×) *xl*; (▽) *xx*; (#) *ll*.

ticles. A yield stress was found in the *lx* and *xx* series, but it was less pronounced in the short delay time samples in the *xl* and *ll* series, and therefore the absence of a yield stress may be related to the graft process.

On the basis of the present evidence and the previously presented dynamic mechanical data, it is concluded that properties in this system are primarily

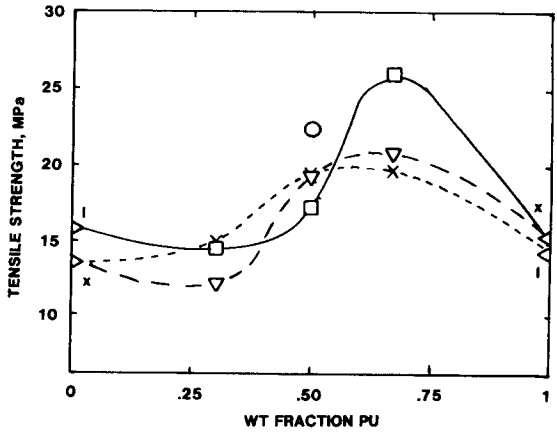

Fig. 11. Maximum tensile strength vs. composition in PU/PBMA mixtures: (□) *lx*; (×) *xl*; (▽) *xx*; (○) *ll*.

dependent on the shape and, to a lesser extent, on the size of the particles in the dispersed phase. Shape and size, in turn, are dependent on the presence or absence of crosslinking in the dispersed phase and on the viscosity of the medium in which it is formed. Much of the property differences between family groups are determined by the proportion of the matrix chains immobilized by the glassy dispersed phase.

References

1. D. J. Moonay and R. B. Fox, *Am. Chem. Soc. Polym. Mater. Sci. Eng. Prepr.*, **58,** 899 (1988).

2. R. B. Fox, D. J. Moonay, J. P. Armistead, and C. M. Roland, *Am. Chem. Soc. Symp. Ser.*, **395,** 245 (1989).

3. R. C. Poller and S. P. Retout, *J. Organomet. Chem.*, **173,** C7 (1979).

4. H. Djomo, A. Morin, M. Damyanidu, and G. Meyer, *Polymer,* **24,** 65 (1983).

5. G. Allen, M. J. Bowden, G. Lewis, D. J. Blundell, and G. M. Jeffs, *Polymer,* **15,** 13 (1974).

6. E. R. Weibel, in Principles and Techniques of Electron Microscopy, M. A. Hayat, Ed., Van Nostrand Reinhold, New York, 1973, Vol. 3, Chap. 6.

7. R. E. Touhsaent, D. A. Thomas, and L. H. Sperling, *Am. Chem. Soc. Adv. Chem. Ser.*, **154,** 206 (1976).

8. K. C. Frisch, D. Klempner, S. Migdal, and H. L. Frisch, *J. Polym. Sci. Polym. Chem. Ed.*, **12,** 885 (1974).

Received July 10, 1989
Accepted January 3, 1990